Electronic Supplementary Information

Article "Synthesis, Structure and Electrochemical Performance of Ultra-High-Entropy Rare Earth Orthoferrite (UHE REO) for Overall Water Splitting (OWS)"

In this work, X-ray electron spectroscopy (XPS) was performed using an ESCALAB 250Xi spectrometer (Thermo Fisher Scientific, USA) with Al Kα radiation. The obtained spectra were fitted using the Voigt fitting method via the Fityk software. The resulting data are shown in **Table S1** and **Fig. S1**.

Table S1. Values of binding energy, spin-orbit splitting energy, and corresponding oxidation state of UHE REO's constituent elements

№	Elements	Orbitals	Binding energy peaks, eV	Spin-orbit splitting energy, eV	Oxidation state
1	Sc	$2p_{3/2}$	401	5	+3
		$2p_{1/2}$	406		
2	Y	$3d_{5/2}$	157	2	+3
		$3d_{3/2}$	159		
3	La	$3d_{5/2}$	834	17	+3
		$3d_{3/2}$	851		
4	Ce	$3d_{5/2}$	885	16	+4
		$3d_{3/2}$	901		
5	Pr	$3d_{5/2}$	932	18	+3
		$3d_{3/2}$	950		
6	Nd	$3d_{5/2}$	974	21	+3
		$3d_{3/2}$	995		
7	Sm	$3d_{5/2}$	1082	23	+3
		$3d_{3/2}$	1105		
8	Eu	$3d_{5/2}$	1132	32	+3
		$3d_{3/2}$	1164		
9	Gd	$3d_{5/2}$	1186	35	+3
		$3d_{3/2}$	1221		
10	Tb	$3d_{5/2}$	1246	28	+3
		$3d_{3/2}$	1274		
11	Dy	$3d_{5/2}$	1300	30	+3
		$3d_{3/2}$	1330		
12	Ho	4d	161	–	+3
13	Er	4d	168	–	+3
14	Tm	4d	176	–	+3
15	Yb	4d	185	–	+3
16	Lu	$4d_{5/2}$	196	10	+3
		$4d_{3/2}$	206		

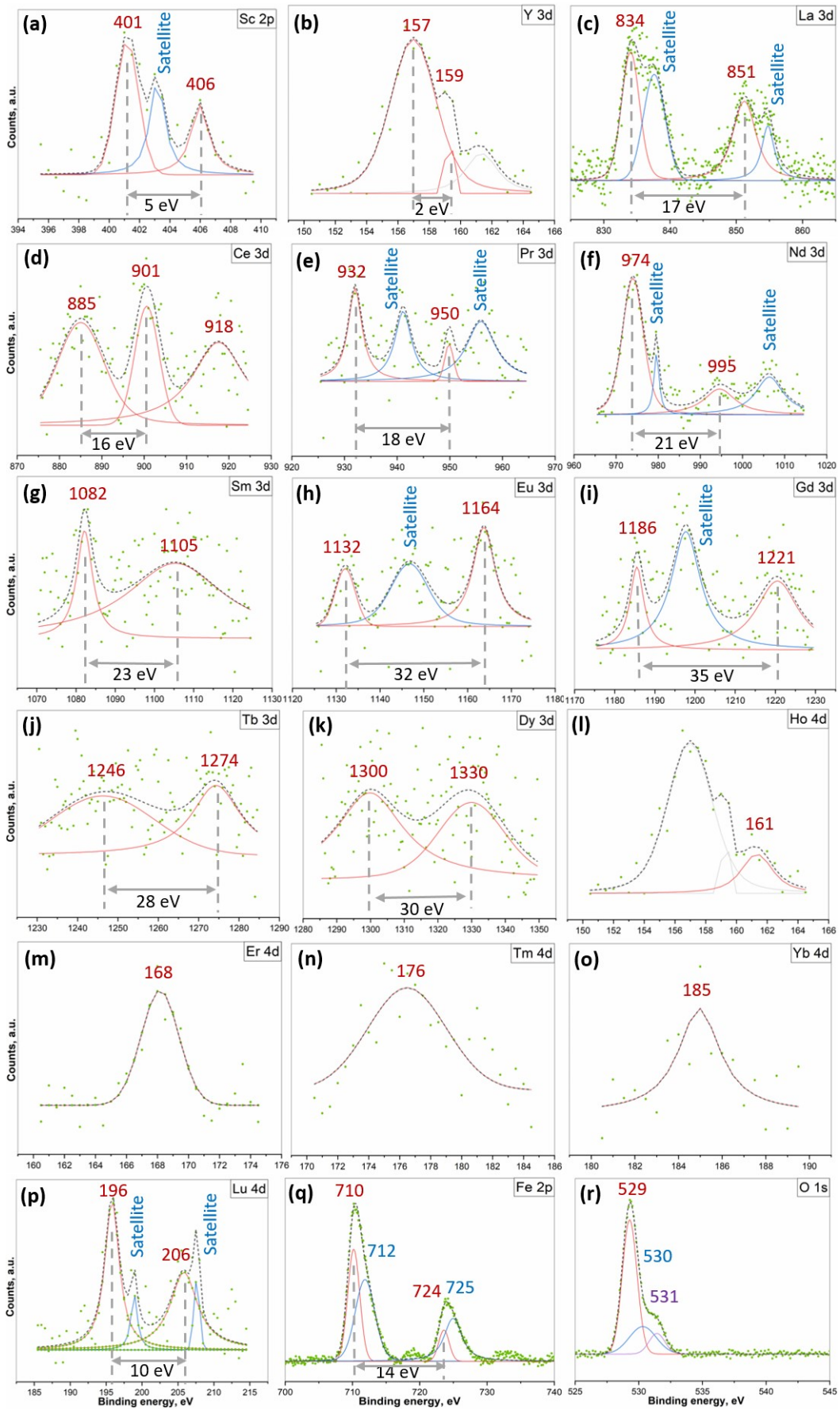
(a)
Sc 2p
401
Satellite
406
5 eV
(b)
Y 3d
157
159
2 eV
(c)
La 3d
834
Satellite
851
Satellite
17 eV
(d)
Ce 3d
885
901
918
16 eV
(e)
Pr 3d
932
Satellite
950
Satellite
18 eV
(f)
Nd 3d
974
Satellite
995
Satellite
21 eV
(g)
Sm 3d
1082
1105
23 eV
(h)
Eu 3d
1132
Satellite
1164
32 eV
(i)
Gd 3d
1186
Satellite
1221
35 eV
(j)
Tb 3d
1246
1274
28 eV
(k)
Dy 3d
1300
1330
30 eV
(l)
Ho 4d
161
(m)
Er 4d
168
(n)
Tm 4d
176
(o)
Yb 4d
185
(p)
Lu 4d
196
Satellite
206
Satellite
10 eV
(q)
Fe 2p
710
712
724
725
14 eV
(r)
O 1s
529
530
531
Counts, a.u.
Binding energy, eV

Fig. S1. XPS profiles of UHE REO's constituent elements: Sc 2p (**a**), Y 3d (**b**), La 3d (**c**), Ce 3d (**d**), Pr 3d (**e**), Nd 3d (**f**), Sm 3d (**g**), Eu 3d (**h**), Gd 3d (**i**), Tb 3d (**j**), Dy 3d (**k**), Ho 4d (**l**), Er 4d (**m**), Tm 4d (**n**), Yb 4d (**o**), Lu 4d (**p**), Fe 2p (**q**), and O 1s (**r**).

The characteristic values of binding energy (BE) peaks and spin-orbit (S-O) splitting energy of the compound's individual rare earth element are listed in **Table S1**. As can be seen, almost all rare earth metals in the UHE REO have a trivalent oxidation state [1–4]. However, there are some exceptions, such as the fact that the Ce element exists primarily in the +4-oxidation number [5]. Furthermore, for the Fe 2p XPS profile (see **Fig. S1-q**), the BE peaks centered at 710, 724 eV and 712, 725 eV belong to the oxidation states of Fe(II) and Fe(III), respectively [6]. For the O 1s XPS profile (**Fig. S1-r**), the BE peaks observed at 529, 530, and 531 eV can be attributed to lattice oxygen, defective oxygen, and surface-adsorbed oxygen, respectively [7,8].

Reference

[1] M.H. Joo, S.J. Park, S.-M. Hong, C.K. Rhee, D. Kim, Y. Sohn, Electrodeposition and Characterization of Lanthanide Elements on Carbon Sheets, Coatings. 11 (2021) 100. https://doi.org/10.3390/coatings11010100.

[2] R. Rahman, J.P. Klesko, A. Dangerfield, M. Fang, J.-S.M. Lehn, C.L. Dezelah, R.K. Kanjolia, Y.J. Chabal, Mechanistic study of the atomic layer deposition of scandium oxide films using $Sc(MeCp)_2(Me_2pz)$ and ozone, J. Vac. Sci. Technol. A Vacuum, Surfaces, Film. 37 (2019). https://doi.org/10.1116/1.5059695.

[3] L. Mariscal-Becerra, R. Vázquez-Arreguín, U. Balderas, S. Carmona-Téllez, H. Murrieta Sánchez, C. Falcony, Luminescent characteristics of layered yttrium oxide nano-phosphors doped with europium, J. Appl. Phys. 121 (2017). https://doi.org/10.1063/1.4979209.

[4] P. Misra, S.P. Pavunny, Y. Sharma, R.S. Katiyar, Resistive Switching and Current Conduction Mechanisms in Amorphous $LaLuO_3$ Thin Films Grown by Pulsed Laser Deposition, Integr. Ferroelectr. 157 (2014) 47–56. https://doi.org/10.1080/10584587.2014.911633.

[5] A. Sarkar, C. Loho, L. Velasco, T. Thomas, S.S. Bhattacharya, H. Hahn, R. Djenadic, Multicomponent equiatomic rare earth oxides with a narrow band gap and associated praseodymium multivalency, Dalt. Trans. 46 (2017) 12167–12176. https://doi.org/10.1039/C7DT02077E.

[6] F. Han, L. Ma, Q. Sun, C. Lei, A. Lu, Rationally designed carbon-coated Fe_3O_4 coaxial nanotubes with hierarchical porosity as high-rate anodes for lithium ion batteries, Nano Res. 7 (2014) 1706–1717. https://doi.org/10.1007/s12274-014-0531-y.

[7] Y. Zhu, L. Zhang, B. Zhao, H. Chen, X. Liu, R. Zhao, X. Wang, J. Liu, Y. Chen, M. Liu, Improving the Activity for Oxygen Evolution Reaction by Tailoring Oxygen Defects in Double Perovskite Oxides, Adv. Funct. Mater. 29 (2019) 1–12. https://doi.org/10.1002/adfm.201901783.

[8] J. Tapia-P, J. Gallego, J.F. Espinal, Calcination Temperature Effect in Catalyst Reactivity for the CO SELOX Reaction Using Perovskite-like $LaBO_3$ (B: Mn, Fe, Co, Ni) Oxides, Catal. Letters. 151 (2021) 3690–3703. https://doi.org/10.1007/s10562-021-03601-z.